Characterizing Network Architecture for Inter-satellite Communication and Relative Navigation in Precise Formation Flying

Rui Sun, Jian Guo, Eberhard Gill, Daan Maessen
Chair of Space Systems Engineering, Faculty of Aerospace Engineering
Delft University of Technology
Kluyverweg 1, 2629 HS, Delft, the Netherlands
r.sun@tudelft.nl

***Abstract*—Precise formation flying (PFF) missions require formation acquisition and maintenance through interactions among spacecraft by inter-satellite communication and relative navigation. That requires the network architecture to satisfy dedicated system constraints of time-criticality for updating navigation measurements and flexibility for implementation across various phases of mission operations. Potentially applicable architectures that combine different multiple access technologies, half-duplex/full duplex configurations, and network topologies are discussed and evaluated. Half-duplex CDMA with roles rotating among all spacecraft is shown more suitable and efficient for PFF missions. Its limitation in terms of multiple access interference is analyzed as well.**

Keywords - precise formation flying; communication; relative navigation; time-critical; various mission phases; CDMA

I. INTRODUCTION

Precise formation flying (PFF) missions involve the acquisition and maintenance of spacecraft in a desired relative geometric configuration, especially when trying to create a large virtual spaceborne instrument, such as telescope or interferometer. Coordinating the components of such instruments on separate spacecraft can require highly accurate relative orientation and positioning.

The common way to perform such PFF missions is to use differential Global Navigation Satellite System (GNSS) by exchanging GNSS-based navigation measurements via inter-satellite links [1]. Yet this method is limited to low earth orbit (LEO). Many missions such as PROBA-3, Darwin and TPF require the spacecraft flying in high earth orbit (HEO) or Lagrange points, where GNSS signals are very weak or not available at all [2]. As a result, a dedicated formation flying radio frequency (RF) technique using locally generated inter-satellite ranging signals is necessary. It is expected to integrate with inter-satellite communication for system efficiency. Thanks to the widespread use of spread spectrum techniques, RF signals modulated with a pseudo random noise (PRN or PN) code appears to be advantageous in such integrated system, since they allow both reliable communication and accurate ranging measurements [3].

In considering the properties of communication and ranging driven PFF network, interactions among spacecraft should satisfy system constraints including time-criticality of updating measurements, and flexibility for implementation across various phases of mission operations. This paper will address these constraints, and propose potentially applicable architectures that use fixed assignment for all possible connections by multiple access (MA) technologies. The applicable combinations among different MA, half-duplex/full duplex configurations, and network topologies are discussed and evaluated.

The paper is organized as follows. In Section II, the inter-satellite communication and relative navigation sensor is introduced in order to propose the dedicated constraints for PFF network in Section III. Candidate network architectures and their comparison are presented in Section IV. Network capability in terms of multiple access interference is analyzed in Section V. Section VI concludes the paper and discusses future directions.

II. INTER-SATELLITE COMMUNICATION AND RELATIVE NAVIGATION SENSOR

An inter-satellite sensor for PFF missions is under development that should integrate communication and relative navigation into one package. The method traces heritage to GPS-like technology and is expected to satisfy the following specific high-level requirements:

- Communication and relative navigation are integrated into one package, with mass less than 2 kg, and power consumption less than 2 W;
- Operating range less than 30 km;
- Omni-directional (4π steradian) coverage;
- Flexible to implement across various phases of mission operations in two modes: coarse-mode during the deployment, reconfiguration and collision avoidance tasks; fine-mode during the formation maintenance process;
- Navigation accuracy is 1 m for coarse-mode using code measurement (pseudorange) only, and 1 cm for fine-mode using the combination of code and carrier phase measurements;
- Resolution of related integer ambiguity problem of carrier phase measurement;
- Measurement update rate ≥ 1 Hz.

The inter-satellite sensor functional block diagram is in Fig. 1. Software-defined transceiver is used, in which way the signal generation and processing is accomplished via a programmable microprocessor e.g. FPGA or DSP. The current transceiver version implements the signal generation and processing on PC via Matlab/Simulink.

As shown in Fig. 1, the software-defined transceiver comprises the transmitter and receiver front-end part and

 ISBN: 978-1-61208-128-1

signal simulator and processing part. The front-end is based on hardware design that comprises signal amplifier, band pass filter, down-conversion, sampling, and quantization. The signal simulator and processing are realized only based on software through the signal generation module to generate carrier and PRN code modulated signal, and acquisition, tracking and decoding modules for data recovery, code and carrier phase extraction, and pseudorange (-rate) derivation.

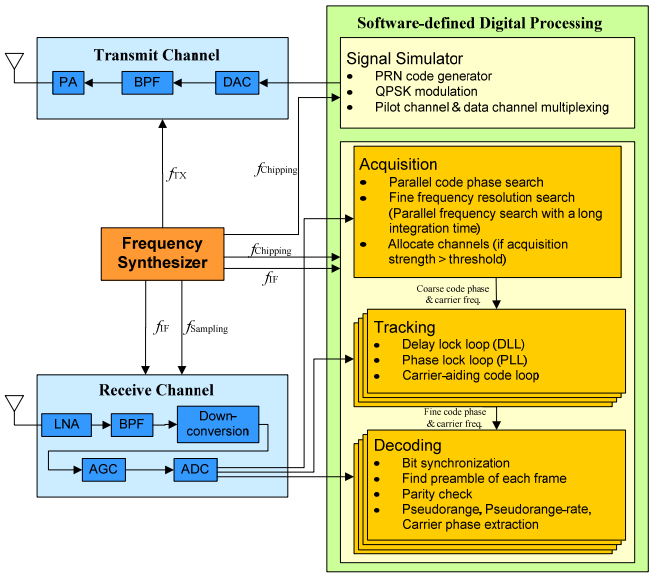

Figure 1. Inter-satellite sensor functional block diagram

Fig. 2 depicts the signal generation and processing simulation results assuming that intermediate frequency (IF) is 9.55 MHz and a sampling rate is 38.19 MHz. In signal simulator, PRN code is generated with a chipping rate of 10.23 Mcps and length of 1023 chips. Compared to GPS C/A code, such signal can increase the theoretical lower bound of code tracking accuracy of approximately 3 times better at the same noise level and same front-end bandwidth according to the Cramér-Rao lower bound theory [4]. Doppler shift is generated following a linear function.

The process of acquisition is a global search in a two dimensional search space for approximate values of Doppler shift and code phase. This process is time and computation consuming. Therefore, parallel code/frequency one-dimensional search using Fast Fourier Transform (FFT) is implemented. After acquisition, control is handed over to delay lock loop (DLL) and phase lock loop (PLL), which yield fine estimates of code and carrier phase continuously and track the variations due to dynamics between satellites. Communication bits can be extracted from the tracking loops. Pseudorange measurements are derived afterwards.

III. CONSTRAINS ON PFF NETWORK ARCHITECTURE

A. *Time-critical requirements*

Time-critical requirements are driven by the nature of dynamic relative navigation process that contains two steps: propagation in the filter and measurement update.

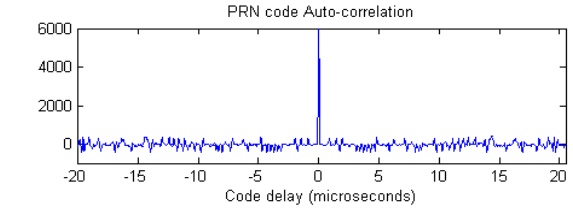

(a) Auto-correlation, chipping rate is 10.23 Mcps

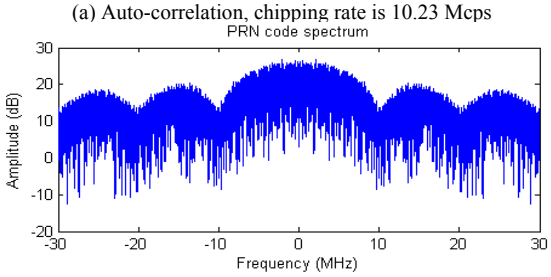

(b) Code Spectrum, chipping rate is 10.23 Mcps

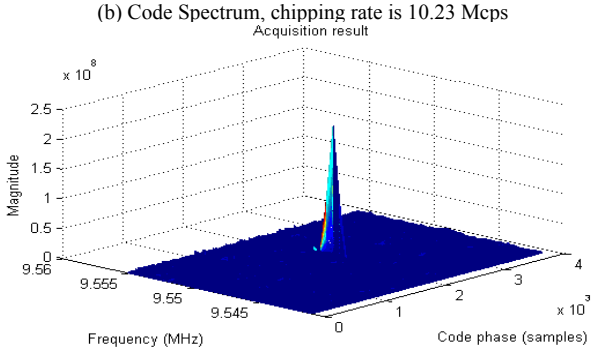

(c)) Acquisition results, the peak is present at the point where the code offset is at 2100 sample (3819 samples in total for one PRN sequence) and carrier frequency is at 9.54904 MHz (that is, Doppler offset at 1038 Hz)

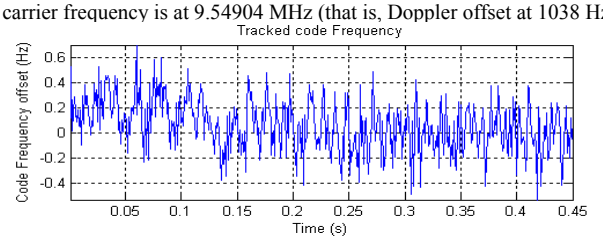

(d) Code frequency offset in DLL

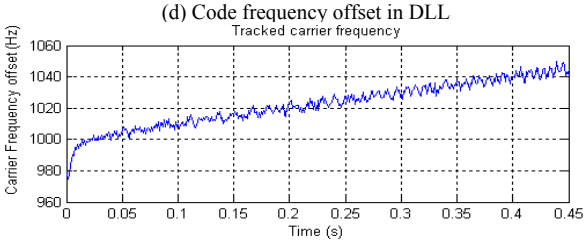

(e) Carrier frequency offset in PLL

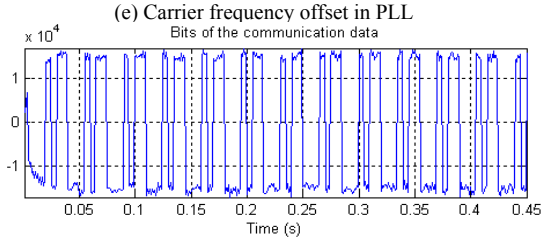

(f) Communication bits extraction. The values are not ±1 because of the quantization in the front-end and integration in the tracking loops.

Figure 2. Software-defined signal generation and processing results

 ISBN: 978-1-61208-128-1

Relative navigation filter (e.g. extended Kalman filter) is used to account for the relative position errors resulting from all relevant non-modeled accelerations acting on the spacecraft. This process employs a numerical integration scheme in the filter that is updated at discrete intervals (t_i) as illustrated in Fig. 3. The estimated relative state vector is obtained from an interpolation of the previous cycle. Based on all the measurements between t_i and t_{i+1}, a continuous polynomial representation of the trajectory is made available, which serves as starting point for the next filter update and relative orbit prediction [5]. Obviously the propagation period t_i-t_{i-1} has to be small if better approximations of relative state vectors are required. On the other hand, t_i-t_{i-1} is limited by the processing time Δt_{proc}. Its typical value is 30 s for low earth orbits. While in deep space, this period can be extended to several minutes.

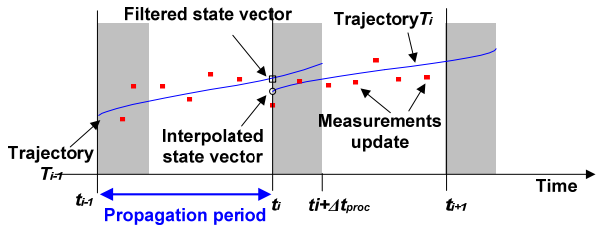

Figure 3. Timeline of relative navigation filter [5]

The measurements used in the filter are provided by the inter-satellite sensor. They can be unambiguous coarse code measurements or ambiguous precise carrier phase measurements. Fig. 4 gives their measurement update timelines. The biggest difference between these two timelines is the extra time for integer ambiguities, which should be initialized before using carrier phase to provide precise measurements. The method used by PRISMA mission is to rotate a spacecraft for solving line-of-sight (LOS) ambiguity problem firstly and then distance ambiguity afterwards, taking 5 mins and 10 mins, respectively. The resolution is combined with tabulated multipath correlation through a filtering and smoothing process [6].

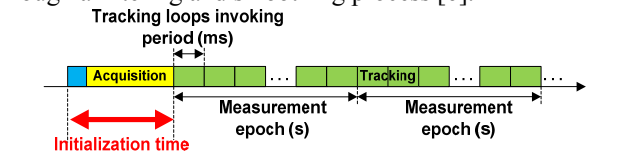

(a) Timeline of code measurement generation

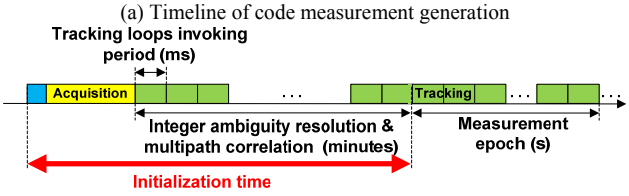

(b) Timeline of carrier phase measurement generation

Figure 4. Timeline of code and carrier phase measurements generation

B. *Flexible operations across all mission phases*

Another important consideration in PFF network is to recognize that the relative navigation requirements may change during the course of the mission's operations. Inter-satellite sensor is expected to operate across various phases of formation precision, requiring different levels of position sensing and control maneuvering as shown in Fig. 5. A connectivity index table (CIT) is proposed to be part of traffic exchanged among spacecraft to share the current network condition. The measured range can also be filled in CIT, in which way a spacecraft can know where the others are even though not all of them are directly connected.

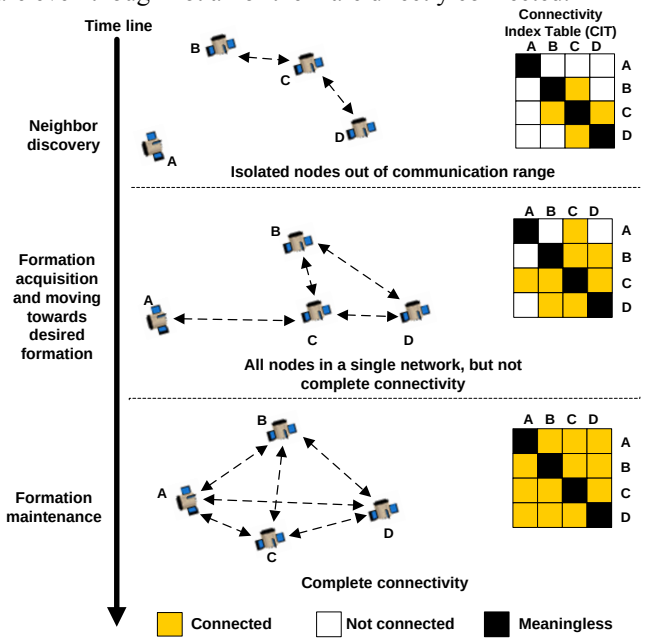

Figure 5. Evolutionary phases of a PFF mission

In the initial deployment where spacecraft may be separated by substantial distances from one to another, the resolution of position and orientation data are based perhaps on coarse-mode sensors using code measurements only for collision avoidance and enabling further movement toward the desired configuration. Some spacecraft are possibly out of communication range of others as shown in the top of Fig. 5. As the spacecraft continue to aggregate into the desired spatial arrangement, they will eventually discover other spacecraft. This condition is defined as formation acquisition and depicted in the center of Fig. 5. Finally, when all spacecraft are in a "complete connectivity" and settled into the desired pattern, formation maintenance is performed as shown in the bottom of Fig. 5. A much greater degree of positional knowledge is acquired by switching the inter-satellite sensors into the fine-mode to facilitate science operations such as multi-point observation.

IV. NETWORK ARCHITECTURE FOR PFF

As a result of time-critical demands, networking solutions prefer the network nodes in a fixed assignment for all possible connections by multiple access (MA) technologies TDMA, CDMA, FDMA or their combinations, since they enable each spacecraft providing measurements from each of the others equally and timely [3]. Before discussing network architectures, choices of half-duplex/full-duplex configurations and centralized/distributed topologies need to be considered.

 ISBN: 978-1-61208-128-1

Inevitably, if transmitting and receiving happen at the same time, some of the transmitted signal will leak into the receiver front ends and may easily saturate the receiver front ends or otherwise overwhelm the external signals. Half-duplex transceiver enables the transmitter and receiver taking turns to work, in which way "self-signals" are avoided. Full-duplex transceiver uses an appropriate filter to isolate the transmitter and receiver at their separated frequency bands to reject "self-signals". If the navigation measurements are not required simultaneously and continuously, half-duplex configuration is adequate and power-saving.

Network topology is expected to operate in a flexible arrangement, so as to account for the evolutionary phases of a PFF mission as shown in Fig. 5. Neither solely centralized nor distributed topology is efficiently applicable during the neighbor discovery and formation acquisition phases, because some spacecraft are possibly out of communication range of others and could not access to the network. As the spacecraft progress towards the desired formation, it is better for the topology to evolve to a centralized graph in order to enable at least one spacecraft as reference for precise relative navigation and formation control. The role of reference can rotate from one spacecraft to another to avoid the problem of single point of failure.

Roles rotating at different time slots will give a robust and efficient connectivity. It can be implemented in a TDMA sequence with a strict timing boundary or a CDMA configuration with an adjustable period of time slot. Constraints of operating any of them come from the time-critical navigation requirements. Details will be explained in the following parts taking four spacecraft for example.

A. *Half-duplex TDMA*

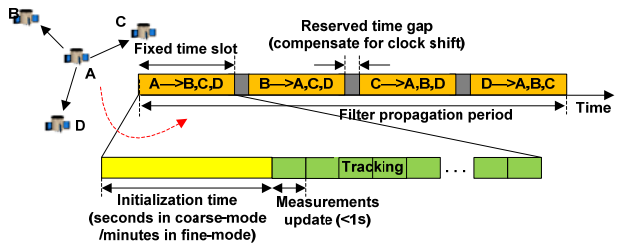

Figure 6. Half-duplex TDMA

A half-duplex TDMA architecture is illustrated in Fig. 6. It should be noted that the onboard relative navigation filters for a certain spacecraft are expected to propagate using complete measurements from all of the other spacecraft. In TDMA mode, these measurements are given in different time slots. Therefore, the time slot is limited by the filter propagation period. That is, if a complete duty cycle of one TDMA sequence is as long as propagation period t_i-t_{i-1}, time slot will be one-quarter (1/number of spacecraft) of t_i-t_{i-1}, or even smaller to compensate for clock drift by reserving a time gap between two time slots. During each time slot, the roles of spacecraft rotate, thus the signals should be re-acquired. Signal re-acquisition takes long time and has the possibility of exceeding the filter propagation period, especially when implementing carrier phase measurement and associated integer ambiguity re-initialization.

Under such circumstances, choosing time slot is in a dilemma, unless the time-critical constraint is loosened by increasing the propagation period or limiting the re-acquisition time. It is possible to extend the propagation period, or equivalently let the filter freely propagate without measurement updates, however, at the expense of an increase of the relative navigation error. Otherwise, it is promising to shorten initialization time through a rapid integer ambiguity resolution instead of maneuvering spacecraft in long time.

Apart from the time-critical constraint, another limitation of TDMA scheme is the need of time synchronization. Inevitably, the clock drift makes time unsynchronized on different spacecraft. An easy way to reduce its influence on TDMA is to reserve a time gap between two time slots in order to compensate for clock drift. However, it involves the risk that the drift may exceed time gap.

B. *Half-duplex CDMA with roles rotating*

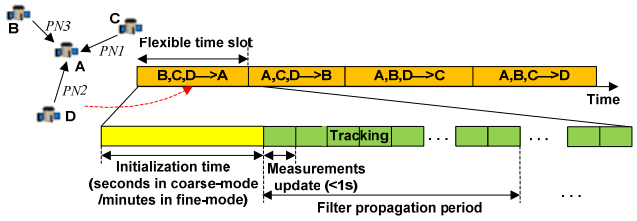

Figure 7. Half-duplex CDMA with roles rotation

Half-duplex CDMA with roles rotating architecture poses better capability than TDMA as show in Fig. 7. For a certain spacecraft, complete measurements from all of the other spacecraft are obtained in the same time slot simultaneously, which makes the duration of time slot much more flexible. It can be long enough to account for propagation period and re-acquisition time. The time slot is also adjustable during the implementation to enable code or carrier phase measurements at different mission phases. In addition, the signals transmitted from other spacecraft are not necessary to start at the same time, because the duration of a time slot can be relatively long and tolerant if one spacecraft is joining in or dropping out of the formation. It is applicable if assigning different time slots for different spacecraft, which happens when a spacecraft needs following long time measurement updates to precisely estimate the relative trajectory change e.g. in a maneuver operation, while others do not.

Some limitations of this concept also exist. The use of CDMA structures results in the well-known near-far problems when different separation distances between spacecraft cause various signal power levels at the receiver. CDMA performance will be discussed in the next section.

C. *Full-duplex CDMA in centralized topology*

As comparison, another candidate architecture using full-duplex CDMA in centralized topology is introduced as shown in Fig. 8. Isolation between transmitter and receiver is realized by separated frequencies and appropriate filters. The measurements can be generated simultaneously and continuously, taking the advantage of permitting ranging signals passed between spacecraft without the necessity of re-acquisition each time at different time slots. Time-critical

 ISBN: 978-1-61208-128-1

requirement is satisfied in an extreme solution that is continuous connectivity. Besides, this method brings its unique benefit that both clock offset and relative distance can be yielded using dual one-way ranging [7].

However, the flexibility is low because it uses centralized topology. Otherwise, full connectivity is possible by CDMA/FDMA combination, but at the expense of high complexity of sensor design with multi-frequency transmitter and multi-frequency multi-channel receiver.

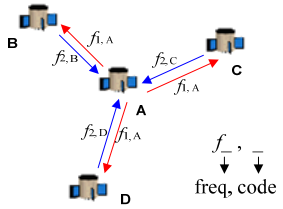

Figure 8. Full-duplex CDMA

D. Evaluation of different architectures

To evaluate different architectures, weighted criteria are given in Table I from 1 to 5 based on the degree of importance to balance mission operations and design cost. Candidate architectures are scored from 1 to 3 to show their capability to satisfy each criterion. The scores for the former three criteria are self-explanatory according to the analysis indicated above. Regarding power consumption, as a rule of thumb, a half-duplex transceiver consumes less power than a full-duplex one; the transmitter consumes more power than the receiver. Therefore, for a half-duplex TDMA architecture which arranges one spacecraft in transmit-mode while the others are in receive-mode, power consumption is the lowest. Full-duplex CDMA is the most power consuming one. With respect to system complexity criterion, TDMA based on simple timing logic access strategy is easier to implement than multi-channel PRN-based CDMA; Half-duplex configuration simplifies the system by switching transmitter and receiver to reject self-signal instead of using complex filters at separated frequencies in full-duplex configuration.

By calculating the score results for different architectures in Table I, half-duplex CDMA with roles rotating is the best-suited architecture for PFF missions.

TABLE I. COMPARISON OF DIFFERENT POTENTIALLY APPLICABLE NETWORKING ARCHITECTURES

Weighted Criteria		**Candidate Network Architectures**		
		Half-duplex TDMA	***Half-duplex CDMA with roles rotating***	***Full-duplex CDMA***
Tolerance of time-critical constraint	5	1	2	3
Flexibility to support various mission phases	4	2	3	1
Scalability to enable s/c joining in or dropping out of the formation	1	1	3	2
Low Power consumption	3	3	2	1
Low System complexity	2	3	2	1
$\sum$ *weight * score*		29	36	26

V. CDMA PFF NETWROK CAPABILITY: MULTIPLE ACCESS PERFORMANCE AND NEAR-FAR PROBLEM

The multiple access capability of CDMA can be achieved by using spread spectrum orthogonal signals. However, a completely orthogonal signaling is not possible, which means cross-correlations are nonetheless present and induce noise in terms of multiple access interference (MAI).

Assume that there are two signals, which are all un-correlated PRN codes with identical spectrum $G_s(f)$ and received at the same power level of P_s. The MAI term is introduced due to cross-correlation between undesired signal $c_m(t)$ and desired reference signal $c_k(t)$, where $c(t)$ represents PRN code. Ignoring the data modulation, Doppler frequency differences and noise for the moment, the MAI term is $c_m(t-\tau_m)c_k(t-\tau_k)$ with code delay τ_m, τ_k. Its power spectrum $G_{MAI}(f)$ is thus obtained by convolving the individual signal spectrum $G_s(f)$ [8]:

$$G_{MAI}(f) = P_s \int G_s(f) G_s(v-f) dv \quad (1)$$

Only the MAI spectrum near $f=0$ is important because the correlation filters have a very small bandwidth. $G_s(f)$ is in the form of $sinc^2$, thus [8]:

$$G_{MAI}(0) = P_s \int G_s^2(v) v = P_s \int_0^\infty \left(\frac{\sin \pi f / f_c}{\pi f / f_c} \right)^4 df = \alpha P_s / f_c \quad (2)$$

where f_c is chipping rate, α is a coefficient as a function of the filtered spectrum of $sinc^2$. If the spectrum includes all of its sidelobes, α is 2/3. If the spectrum is filtered to include only the mainlobe, α increases to approximately 0.815 [8].

Assuming M spacecraft in the formation, all of exactly at the same separation distances, $M-1$ interfering multiple access signals exist. Considering white noise with noise spectrum density of N_0, the equivalent noise density and the effective energy per bit to equivalent noise density ratio are:

$$N_{0eq} = N_0 + \alpha(M-1)P_s / f_c \quad (3)$$

$$\frac{E_b}{N_{0eq}} = \frac{P_s T_d}{N_0 + \alpha(M-1)P_s / f_c} \quad (4)$$

where $T_d = 1/f_d$, f_d is data bit rate. E_b/N_{0eq} determines the bit error rate. It is on the order of 10 dB if BER=10^{-5} and BPSK modulation without error correction coding is employed.

Furthermore, if we take into account of the various separation distances between spacecraft during operations, the near-far problem shows up in which the effective E_b/N_{0eq} from a remote transmitter is further reduced due to the increase of MAI from a transmitter in close proximity. Because the received power is inversely proportional to the square of distance, MAI spectrum density in eq. (2) is consequently multiplied by a factor of R_f^2/R_n^2, which means the far desired signal to near undesired interferences range-squared ratio. E_b/N_{0eq} can then be revised to:

$$\frac{E_b}{N_{0eq}} = \frac{P_s T_d}{N_0 + \alpha(M-1)(R_f^2 / R_n^2)P_s / f_c} = \frac{P_s}{N_0 f_d \beta} \quad (5)$$

The multiple access effect of M-1 near interferences degrades the equivalent noise density by a factor of $\beta = 1 + \alpha(M-1)(R_f^2 / R_n^2)P_s / (f_c N_0)$. Fig. 9 displays the

energy per bit to noise ratio reduction effects of MAI. Assume that Gold code chipping rate f_c is 10.23 Mcps, data bit rate f_d is 2 kbps, and coefficient α is 0.815 using front-end filter with bandwidth of 20 MHz to only filter mainlobe spectrum. Note that signal to noise ratio is at least satisfied to $P_s / N_0 = f_d * E_b / N_0 = 43$ dB when E_b/N_0 is 10 dB.

In the case of a small scale network and small distance diversity, this degradation can be negligible. However, in reality, a wide range of satellite distances exists, especially during the initial deployment phase. According to communication link budget, E_b/N_0 is a distance dependant parameter. The impact of E_b/N_0 degradation can further be translated to the reduced maximum operating range or reduced maximum achievable number of spacecraft.

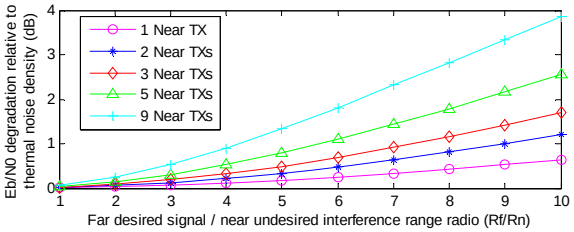

Figure 9. Energy per bit to noise ratio degradation effect resulting

The aforementioned results are based on the assumptions that code spectrum has the form of $sinc^2$ and Doppler frequency differences are ignored. However, the code is not continuous but 1023 chip length sequence periodically repeated every 0.1 ms, which means that the spectrum is made up of 10 kHz ($f_c/P=10.23Mcps/1023$) separated lines following $sinc^2$ envelop [8]. The impact of the existing line components in the spectrum makes the MAI performance much worse than indicated above.

The presence of cross-correlations is the essential reason for MAI. The normalized cross-correlations between pairs of Gold codes have three different spurious peaks taking on values as the following equations with probabilities of 0.75, 0.125 and 0.125, respectively [9]

$$R^{(k,l)}(\tau = iT_c) \in \left\{ \frac{-1}{P}, \frac{-2^{[(n+2)/2]}-1}{P}, \frac{2^{[(n+2)/2]}-1}{P} \right\} \qquad (6)$$

where R is cross-correlation, $T_c=1/f_c$, n is number of shift register stages, and $P = 2^n - 1$ is code length. For Gold code of length 1023, spurious peaks are -65/1023, -1/1023 and 63/1023. The strongest and average peaks are approximately -24 dB and -30 dB, respectively, relative to the main auto-correlation peaks. This limits the dynamic range of a typical receiver employing these spreading codes to 24dB at worst case if only taking one interference transmitter for example. Multiple transmitters will further decrease this level.

If Doppler frequency difference $\Delta f_{m,k}$ and phase difference $\Delta\phi_{m,k}$ are taken into account, cross-correlation term turns to $c_m(t-\tau_m)c_k(t-\tau_k)\cos(2\pi\Delta f_{m,k}t + \Delta\phi_{m,k})$, which produces a line component $\Delta f_{m,k}$ at the spectrum. Ordinarily, the correlation process spreads this line, but the mixing process at the existing code line frequencies results in the interference being minimally suppressed. That is, if Doppler difference is a multiple of line component spacing 10 kHz, MAI noise energy "leaks" through the correlation process, and exacerbates cross-correlation levels to -21.1 dB [8]. Thanks to the code chipping rate increasing to 10.23 Mcps, a 10 kHz Doppler frequency does not occur frequently, relative to 1 kHz line component spacing in C/A code.

VI. Conclusions And Future Work

In this paper, network architecture is presented to support inter-satellite communication and relative navigation for precise formation flying missions. Half-duplex CDMA with roles rotating is selected as a suitable architecture, as it enables system working with a wide range of flexibility, such as enabling both code and carrier phase measurements, allowing to detect some spacecraft while tracking others, and being insensitive to a spacecraft joining in or dropping out of the formation. Its limitation in terms of multiple access interference is also highlighted by analyzing signal cross-correlation performance. It is shown that equivalent energy per bit to noise density ratio is reduced due to the near-far problem, and the limited length of PRN code makes the situation worse at certain Doppler frequency offsets.

The future work includes an improvement of network performance by the following implementations:

Firstly, signal structure will be updated to reduce cross-correlation levels and mitigate multiple access interference.

Secondly, adaptive power control mechanism is useful to accommodate a wide range of inter-satellite distances, as well as minimize the impact of near-far problems.

Thirdly, integer ambiguity problem should be solved rapidly, in order to reduce initialization time, and consequently reduce its impact on time-critical requirements and allow the network in a more flexible manner.

References

[1] R. Kroes, "Precise relative positioning of formation flying spacecraft using GPS", PhD thesis, Delft University of Technology, The Netherlands, 2006.

[2] T. Grelier, A. Garcia, E. Peragin, et al., "GNSS in space: Formation flying radio frequency techniques and technology", Inside GNSS, Jan/Feb, 2009, pp. 43-51.

[3] R. Sun, D. Maessen, J. Guo, and E. Gill, "Enabling inter-satellite and ranging for small satellites", 9th Symposium on Small Satellites Systems and Services, Funchal, Portugal, 31 May – 4 Jun., 2010.

[4] J. Betz, "Binary Offset Carrier Modulations for Radionavigation", Journal of the Institute of Navigation, vol. 48, 2001, pp. 227-246.

[5] E. Gill, O. Montenbruck, K. Arichandran, and S. Tan, "High-precision onboard orbit determination for small satellites-the GPS-based XNS on X-SAT", 6th Symposium on Small Satellites Systems and Services, La Rochelle, France, 20-24 Sep. 2004.

[6] V. Barrena, M. Suatoni, C. Flores, J. Thevenet, and C. Mehlen, "Formation flying RF ranging subsystem for RPISMA: navigation algorithm design and implementation", Proc. 3rd Int. Symposium on Formation Flying, Missions and Technologies, Noordwijk, the Netherlands, 23-25 Apr. 2008.

[7] J. Kim and B. Tapley, "Simulation of dual one-way ranging measurements", Journal of Spacecraft and Rockets, vol. 40, 2003, pp. 419-425.

[8] J. Spilker, "Signal structure and theoretical performance", Global Positioning System: Theory and Applications, Vol. 1, pp. 57-105.

[9] M. Pratap and P. Enge, Global Positioning System: Signals, Measurements and Performance, 2nd ed., pp. 365-379.

 ISBN: 978-1-61208-128-1